Measuring Adapter Efficiency Using a Sliding Short Circuit

WILLIAM C. DAYWITT AND GEORGE COUNAS

Abstract—**This paper describes a simple technique for measuring the efficiency of adapters with losses less than 2dB. The technique is useful in microwave applications where a moderate error in the measured loss is acceptable. This error is less than 10 percent of the loss for losses between 0.5 and 2dB, and is less than 0.05dB below 0.5dB. An expression for the error is given.**

I. Introduction

THERE are many examples in the field of microwave metrology where adapters are used to interconnect components with different connectors, and where accurate knowledge of the adapter efficiency is required but is not readily available or easily measurable. This is an especially vexing situation in calibration laboratories, where measurement accuracy may require a separate standard for every connector type. For example, a waveguide noise source cannot be calibrated directly with a coaxial noise standard because of their different connectors. The obvious solution, attaching a waveguide-to-coaxial adapter to either the standard or the waveguide noise source, requires a measurement of the adapter efficiency in order to complete the calibration. Unfortunately, obtaining an accurate measurement is often difficult or impossible. Even at the National Institute of Standards and Technology Laboratories (NIST), where there is an extensive collection of measurement instrumentation and expertise, it is often difficult to obtain the required measurement. Similar difficulties are encountered in power, attenuation, and antenna measurements.

Existing techniques [1]–[5] for adapter evaluation require considerable effort and are designed to achieve the greatest possible accuracy. In particular, [5] contains a discussion of a highly accurate means of accomplishing the objectives of the present paper using a tuned, fixed-frequency reflectometer. In contrast to these techniques, however, the technique to be described uses approximations that yield accuracies sufficient for most microwave applications, and is relatively simple to perform.

The calibration of a waveguide noise source is illustrated in Fig. 1, where the output noise power P_x of the source is to be calibrated by a coaxial noise power standard. Unfortunately, the waveguide power cannot be compared directly with the coaxial power P_s because the source and standard have different connectors. With a waveguide-to-coaxial adapter attached to the waveguide source as shown in the figure, however, the ratio Y of the powers can be measured by the radiometer, giving (noise generated in the adapter and radiometer have been neglected)

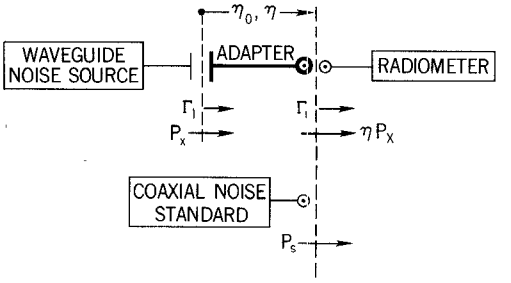

Fig. 1. Schematic drawing of a noise calibration.

$$P_x\eta = YP_s \tag{1}$$

where η is the adapter efficiency (it is a function of the radiometer reflection coefficient Γ_r and approaches 1 as the dissipative loss within the adapter vanishes). If Y and P_s are known, P_x can be obtained from (1) and the calibration completed if the adapter efficiency η can be determined.

A simple technique for determining η using a sliding short circuit (SS) is the subject of this paper. It takes advantage of the fact that η can be factored into the product

$$\eta = \zeta\eta_0 \tag{2}$$

where η_0 is the *intrinsic* adapter efficiency and is a function only of the adapter parameters and not Γ_r. It accounts for the dissipative loss intrinsic to the adapter and approaches 1 as that loss vanishes. The effects of the radiometer reflections may be accounted for by ζ, which is 1 if either the adapter loss or the radiometer reflection coefficient magnitude $|\Gamma_r|$ vanishes. Because of this fact, ζ is close to 1 (see (A15) in Appendix I) and can be discarded in many practical applications, leading to

$$\eta \doteq \eta_0. \tag{3}$$

The following sections of the paper describe a simple and moderately accurate method for measuring η_0, and hence for determining η. It requires an SS and a reflectometer (or an ANA operating in a fixed frequency mode)

Manuscript received August 22, 1989; revised November 6, 1989.

The authors are with the Electromagnetic Fields Division, Center for Electronics and Electrical Engineering, National Institute for Standards and Technology, 325 Broadway, Boulder, CO 80303.

IEEE Log Number 8933249.

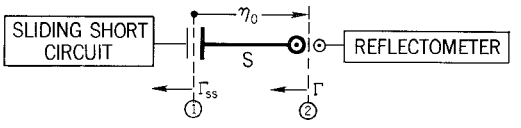

Fig. 2. Schematic drawing of an adapter measurement.

capable of measuring reflection coefficient magnitudes. The measurement procedure for the waveguide-to-coaxial adapter example described above involves calibrating the reflectometer with a coaxial connector as its input port, attaching the adapter to the reflectometer and the waveguide SS to the adapter, and measuring the reflection coefficient magnitudes of the SS/adapter combination as the phase of the SS is varied over approximately half a wavelength. The efficiency is then determined from

$$\eta_0 \doteq \frac{\langle|\Gamma|\rangle}{|\Gamma_{ss}|} \tag{4}$$

where $\langle|\Gamma|\rangle$ is the average of the measured reflection coefficient magnitudes (obtained by the experimental arrangement shown in Fig. 2) resulting from the series of SS phases and where $|\Gamma_{ss}|$ is the known reflection magnitude of the SS. This "known" value must be determined beforehand in the region where the SS shorting element is operated.

The next section describes the theory leading to (4), where two "averaging" methods are discussed, the second of which is of primary interest. A few comments concerning both methods and the determination of $|\Gamma_{ss}|$ end that section. Experimental data supporting the theoretical conclusions are presented in Section III for a waveguide-to-coaxial and a coaxial-to-coaxial adapter. Section IV examines the errors in the technique, with summary and conclusions in Section V. Theoretical details are found in Appendixes I and II.

II. Theory

A measurement of the intrinsic efficiency η_0 is illustrated in Fig. 2. The adapter is connected to a reflectometer that has been calibrated with a coaxial connector at its input port. A waveguide SS is attached to the adapter, the reflection coefficient of which has a known magnitude $|\Gamma_{ss}|$ and a variable phase ϕ that varies as the position of the shorting element in the SS is varied:

$$\Gamma_{ss} = |\Gamma_{ss}|e^{j\phi}. \tag{5}$$

The $\boldsymbol{S}$ shown in the figure is the scattering matrix [6] of the adapter and is used in the appendixes.

The reflection coefficient Γ of the SS/adapter combination can be expressed in the form (Appendix II)

$$\Gamma = A + Be^{j\Psi} \tag{6}$$

where A and B are complex quantities independent of the SS phase ϕ, and where the phase Ψ varies with ϕ. As ϕ is varied the magnitude of Γ in (6) traces a sinusoid that lies between $|B|+|A|$ and $|B|-|A|$. This implies that $|A|$ vanishes and that $|B|$ is 1 for a lossless adapter and an SS with a reflection coefficient magnitude of 1 since $|\Gamma|$ must be 1 for all phases ϕ under these ideal conditions. A $|B|$ of 1 under lossless conditions further implies that $|B|$ is proportional to the intrinsic efficiency of the adapter. These ideas are pursued in Appendixes I and II, where the following approximation is derived:

$$\eta_0 \doteq \frac{|B|}{|\Gamma_{ss}|}. \tag{7}$$

Equation (7) shows that η_0 can be determined by measuring $|B|$ if $|\Gamma_{ss}|$ is known. There are two ways of performing the measurement. The more involved of the two will be discussed first for completeness sake. This will be followed by the simpler technique, which is the subject of this paper and which is used in the next section with the measurement data.

Taking the magnitude squared of (6) leads to (A24):

$$|\Gamma|^2 = |A|^2 + |B|^2 + 2|AB|\cos(\phi_\Gamma - \phi_A) \tag{8}$$

where ϕ_Γ and ϕ_A are the phases of Γ and A respectively. The SS is now varied through 180° in a number of steps, yielding a sequence of values for $|\Gamma|^2$ which can be used in a nonlinear least-squares fitting routine to determine $|A|$, $|B|$, and ϕ_A, as shown below. Using the definitions

$$a \equiv |A|^2 + |B|^2 \tag{9}$$

and

$$b \equiv 2|AB| \tag{10}$$

in (8) leads to

$$|\Gamma|^2 = a + b\cos(\phi_\Gamma - \phi_A) \tag{11}$$

which can be fitted to the sequence of $|\Gamma|^2$ data to determine a, b, and ϕ_A. Using these values with (9) and (10) gives

$$|B| = \frac{\sqrt{a+b} + \sqrt{a-b}}{2} \tag{12}$$

and

$$|A| = \frac{b}{2|B|}. \tag{13}$$

The value of $|B|$ from (12) can now be inserted into (7) to determine η_0. The reflectometer must be capable of measuring the phase of Γ to use this technique. This phase information is not required in the following method.

The simpler technique for determining $|B|$ makes use of the fact that $|A/B| \ll 1$ (Appendix II) and leads to the following approximation of (8):

$$|\Gamma| \doteq |B|\left[1 + \left|\frac{A}{B}\right|\cos(\phi_\Gamma - \phi_A)\right]. \tag{14}$$

If the sequence of $|\Gamma|$ values generated by sliding the short is now averaged (see Fig. 3 and the discussion at the end of this section), (14) leads to

$$\langle|\Gamma|\rangle = |B|\left[1 + \left|\frac{A}{B}\right|\langle\cos(\phi_\Gamma - \phi_A)\rangle\right] \doteq |B| \tag{15}$$

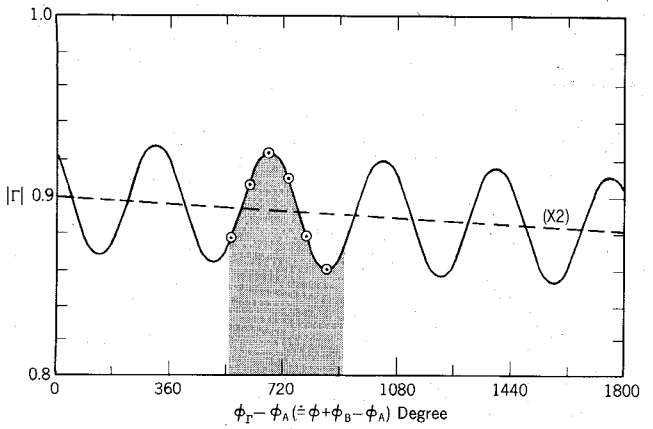

Fig. 3. Simulated reflection coefficient for the adapter/SS combination.

where $\langle \cdots \rangle$ indicates the averaging process. $|A/B|$ is small by virtue of the low-loss nature of the adapter, and $\langle \cos \rangle$ can be made small by proper sliding of the short. Thus, their product is quite small. For example, if the short is slid an even number of times over half of a guide wavelength (e.g. 0, 30, 60, 90, 120, and 150°), then ϕ_Γ will vary over a wavelength (approximately 0, 60, 120, 180, 240, and 300° if ϕ_A is 0), and the second term in (15) will be close to zero. Then, (7) and (15) yield

$$\eta_0 \doteq \frac{\langle |\Gamma| \rangle}{|\Gamma_{ss}|}. \tag{4}$$

This is the desired equation that will be used with the experimental data to determine the adapter efficiency.

A computer-simulated adapter/SS reflection coefficient magnitude for a WR90 waveguide-to-coaxial adapter at 10 GHz is plotted in Fig. 3. The magnitude $|\Gamma|$ is plotted from 0.8 to 1 for a phase change in $\phi_\Gamma - \phi_A$ from 0 to 1800°. This phase change is the result of pulling the SS's shorting plunger away from the adapter (increasing the length of the short) a distance of 2.5 wavelengths, the average slope (exaggerated by a factor of 2) in the curve being caused by the increased line loss due to the longer length of SS line between the connector and the shorting plunger. The sinusoidal variation is due to a nonvanishing $|A/B|$ ratio in (14). The shaded area in the figure corresponds to the 0.5 wavelength distance the plunger is varied for the adapter measurement, where the circles depict a set of six measured data points similar to those mentioned in the previous paragraph. These points are used to calculate the average in (15). $|\Gamma_{ss}|$ is determined with the shorting plunger in this shaded area before the adapter measurements are begun, the small slope due to line loss having an insignificant effect on the result.

A few words should be said about the sinusoidal variations in Fig. 3, although an in-depth discussion concerning reflectometer or ANA errors is beyond the scope of the present paper. The six data points derived from the variations shown in the figure assume no reflectometer error and could, therefore, be used in either (12) or (15) to determine $|B|$. Certain types of reflectometer error vary with $\phi_\Gamma - \phi_a$ in a sinusoidal pattern similar to (15), however, often obscuring the sinusoidal variation associated with the adapter loss and making the determination of $|B|$ by either method ((12) or (15)) open to question. Fortunately, the averaging process leading to (15) and the averaging process inherent in the least-squares fitting giving (12) both tend to average out these types of errors, enabling either method to yield $|B|$, destroying only the determination of $|A|$ by (13). Measurements show that either method gives approximately the same result (usually within one or two thousandths of a decibel), so the method of (15) is clearly preferred since it is easier to perform and since the determination of $|A|$ is lost anyway due to reflectometer errors.

III. Measurements

The theory in the previous text and the appendixes indicate that (4) is an accurate approximation for calculating adapter efficiency by averaging the reflection coefficient magnitude of an SS/adapter combination. A number of experiments were performed to check this conclusion. Highly accurate measurements of low-loss adapters are difficult to obtain at the present time, however, although there are a number of techniques under investigation at NIST and elsewhere for performing this type of measurement. Hence, the following noise temperature [7] comparisons were performed to check the theory in the absence of more accurate adapter measurement methods.

The noise temperature comparisons were performed by measuring the noise temperature of a noise source/adapter combination and then calculating the intrinsic adapter loss $\eta_{0\,\mathrm{dB}}$ with the equation

$$\eta_{0\,\mathrm{dB}} = 10 \log \left(\frac{T_n - T_a}{T_n' - T_a} \right) \tag{16}$$

where

$$\eta_{0\,\mathrm{dB}} \equiv 10 \log \frac{1}{\eta_0} \tag{17}$$

and where T_n' is the measured noise temperature, T_a is the ambient temperature of the adapter, and T_n is the noise temperature of the source attached to the adapter.

Three different types of waveguide-to-coaxial adapters and a type N-to-7 mm adapter were measured. Table I shows the results, where the first column designates the noise standard (with noise temperature T_n) attached to the adapter; the second column designates the coaxial standard used to measure the noise temperature T_n' of the source/adapter combination; the third column designates the various adapters measured (e.g. "W.NF" means a waveguide-to-type-N-female adapter); the fourth column gives the measurement frequency; the fifth column gives the intrinsic loss of the various configurations as measured by the SS technique; and the sixth column gives the comparison error, i.e., the difference between the losses measured by the SS and the noise temperature technique (eq. (16)). The values in the last column should be less than the combined errors of the two measurement techniques

TABLE I
SLIDING SHORT ADAPTER MEASUREMENT RESULTS

Adp Std	Coax Std	Config.	Freq (GHz)	Loss (dB)	Diff. (dB)
90IV8	7mm	W.NF	10.0	0.371	0.016
90IV5	N	W.NM	9.0	0.149	0.016
90IV8	N	W.NM	9.0	0.152	0.005
90IV5	7mm	W.NM.7	11.2	0.141	0.053
SS1	N	7.NM	8.0	0.019	0.014
SS2	N	7.NM	8.0	0.019	0.007

(the SS and the noise techniques), ± 0.056 dB, used in the comparison. The ± 0.056 dB value is derived in the next section. The last column in the table shows that the comparison differences are within the ± 0.056 dB error limit. That is, the measurement results support the theoretical conclusions of the previous section.

IV. ERRORS

The purpose of this section is to estimate the error in the SS measurement of the intrinsic efficiency η_0, and the resulting total error in η which is a combination of the η_0 error and the error in substituting η_0 for η in practical applications.

The derivation of (4) can be retraced through (A20) and (A24) to obtain the following approximation:

$$\eta_0 \doteq \frac{\langle|\Gamma|\rangle}{|\Gamma_{ss}|}\left[1+|S_{11}|^2\left(1-|\Gamma_{ss}|^2\right)-\left|\frac{A}{B}\right|\left\langle\cos\left(\phi_\Gamma-\phi_A\right)\right\rangle\right]. \tag{18}$$

The relative error in η_0 due to setting the second factor in (18) equal to 1 to obtain (4) is

$$\left(\frac{\Delta\eta_0}{\eta_0}\right)_1 = |S_{11}|^2\left(1-|\Gamma_{ss}|^2\right) + \frac{(1-\eta_0)^2+|S_{11}|\left(1-|\Gamma_{ss}|^2\right)}{\eta_0|\Gamma_{ss}|}\left\langle\cos\left(\phi_\Gamma-\phi_A\right)\right\rangle \tag{19}$$

where (A28) has replaced $|A/B|$. The averaged cosine factor is less than 0.2 if the SS is varied in accordance with the prescription in Section II. With this value, (19) gives an error less than ± 0.002 dB for parameters appropriate to the SS waveguide-to-coaxial measurements in the preceding section and an error less than ± 0.0005 dB for the coaxial measurements.

The relative error in measuring η_0 described by (4) due to errors in $\langle|\Gamma|\rangle$ and $|\Gamma_{ss}|$ is

$$\left(\frac{\Delta\eta_0}{\eta_0}\right)_2 = \frac{\Delta\langle|\Gamma|\rangle}{\langle|\Gamma|\rangle}+\frac{\Delta|\Gamma_{ss}|}{|\Gamma_{ss}|} \tag{20}$$

where the two terms on the right side of (20) are the relative errors in $\langle|\Gamma|\rangle$ and $|\Gamma_{ss}|$.

An additional error is added to the previous errors to account for the Γ_r reflection (Fig. 1) from the system to which the adapter is attached. This error is derived from expression (A15) by dropping the 1, and is $\pm 2|\Gamma_r|(1-\eta_0)^2$.

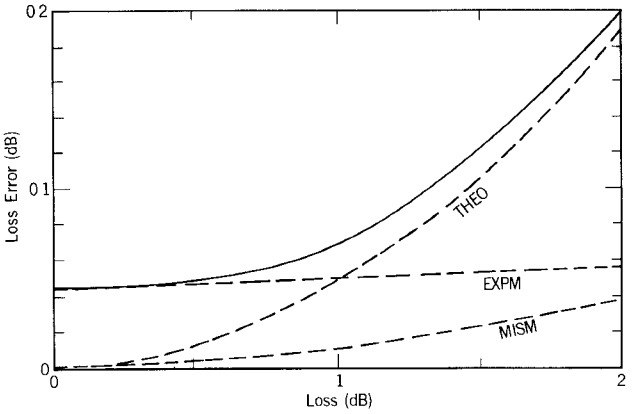

Fig. 4. The absolute loss error as a function of adapter loss.

The total error $\Delta\eta/\eta$ in η is the quadrature sum of the three errors:

$$\frac{\Delta\eta}{\eta} = \left\{\left(\frac{\Delta\eta_0}{\eta_0}\right)_1^2+\left(\frac{\Delta\eta_0}{\eta_0}\right)_2^2+\left[2|\Gamma_r|(1-\eta_0)^2\right]^2\right\}^{1/2}. \tag{21}$$

In summary, the first term in the brackets is the error due to the theoretical approximations leading to (4); the second term is the experimental error; and the last term is the mismatch error due to substituting η_0 for η.

The relative error in (21) expressed in decibels ($4.34\Delta\eta/\eta$) is plotted as the solid curve in Fig. 4 for the following typical values: $|S_{11}| = |\Gamma_x| = 0.03$, $|\Gamma_{ss}| = 0.99$, $\Delta|\Gamma_{ss}| = \Delta\langle|\Gamma|\rangle = 0.005$, and $\langle\cos(\phi_\Gamma - \phi_A)\rangle = 0.2$. This curve represents the error in the decibel loss ($-10*\log\eta$) of the adapter. The THEO, EXPM, and MISM curves are the dB errors obtained from (19), (20), and the last term of (21) respectively. Clearly, the increased error above 1 dB loss is due to a breakdown in the theoretical approximations for adapters with losses above that value. In particular, the magnitude of $|A/B|$ is no longer negligible above the 1 dB loss value. The experimental error dominates below this value.

The relative loss error in percent is plotted in Fig. 5 as a function of the adapter loss. The solid curve corresponding to the total error (21) is less than 10 percent of the loss for adapter losses between 0.5 and 2 dB. The increase below 0.5 dB is due to a relatively constant absolute error being divided by a decreasing loss. The absolute error (Fig. 4) is less than 0.05 dB in this region, however.

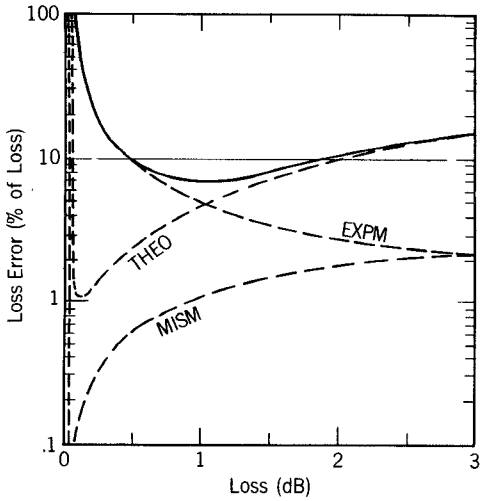

Fig. 5. The relative loss error as a function of adapter loss.

The SS measurements described in the previous section provide an example of (21), where a single six-port reflectometer [8] was used in the reflection coefficient measurements. The $\langle|\Gamma|\rangle$ term produces the largest source of error, ± 0.006, because the reflectometer has a coaxial input for this phase of the measurement. The measurement of the waveguide SS $|\Gamma_{ss}|$ is better, producing a ± 0.004 for the average as the shorting plunger is varied. These give a ± 0.010 experimental error. The adapter was attached to a radiometer with a $|\Gamma_r|$ of 0.1 for the noise measurement portion of the comparison measurements. Assuming a 0.2 dB loss ($\eta_0 = 0.955$) as an average for those measurements, the third therm of (21) gives an error of ± 0.004. The total error is the quadrature sum, or ± 0.011 ($\sqrt{0.002^2 + 0.010^2 + 0.004^2}$) for η. This amounts to a ± 0.047 dB error for η_{dB}.

The error in the noise measurement of $\eta_{0\mathrm{dB}}$ is the quadrature sum of the T_N, T_N', and mismatch errors leading to (16), and is ± 0.030 dB for the adapters described in the previous section. Adding this error in quadrature to the ± 0.047 dB error for determining η_0 indicates that only a ± 0.056 dB or larger comparison error in Section III between the SS and the noise data should be of concern.

V. Summary and Conclusions

A simple method for determining intrinsic adapter efficiency η_0 (eq. (A7)) by measuring the ratio in (4) was discussed in Section II. Appendix I discussed its relationship to the η (A4), which leads to (21) as the total error when using η_0 in place of η. For example, the error is less than ± 0.047 dB for a 0.2 dB adapter attached to a system with a $|\Gamma_r|$ of 0.1.

Loss measurements using the SS and noise techniques were compared in Section III for a number of adapters, with results showing discrepancies less than the ± 0.056 dB sum of the separate experimental errors. This agreement (shown in the "Diff." column of the table) indicates that the SS technique produces the results predicted by the theory and that this technique is useful for efficiency measurements in microwave applications where loss errors of a few hundredths of a decibel are acceptable.

Appendix I

The efficiency η of the adapter in Fig. 1 includes the effects of multiple reflections between the adapter and the radiometer. These reflections slightly modify the efficiency η_0 that the adapter would yield if the radiometer were reflectionless. The magnitude of this modification is investigated here.

The adapter is characterized by its scattering matrix $\boldsymbol{S}$ [6]:

$$\boldsymbol{S} = \begin{pmatrix} S_{11} & S_{12} \\ S_{21} & S_{22} \end{pmatrix}. \tag{A1}$$

The reflection coefficient of the adapter/sliding short combination (Fig. 2) can be expressed as

$$\Gamma = \frac{\sigma\Gamma_{ss} + S_{22}}{1 - S_{11}\Gamma_{ss}} \tag{A2}$$

where

$$\sigma \equiv S_{21}^2 - S_{11}S_{22}. \tag{A3}$$

The adapters under consideration are reciprocal devices ($S_{12} = S_{21}$) so that σ is symmetric under an interchange of the indices "1" and "2." That is, the S_{21}^2 in (A3) could just as well be replaced by S_{12}^2 or $S_{12}S_{21}$.

The adapter efficiency η is related to the scattering coefficients in $\boldsymbol{S}$ and to Γ_r by [6, p. 49]

$$\eta = \frac{(1 - |\Gamma_r|^2)|S_{21}|^2}{(1 - |\Gamma_1|^2)|1 - S_{22}\Gamma_r|^2} \tag{A4}$$

where Γ_1 and Γ_r are defined in Fig. 1. Equation (A4) can be written in the form

$$\eta = \zeta\eta_0 \tag{A5}$$

by using the definitions

$$\zeta \equiv \frac{(1 - |\Gamma_r|^2)(1 - |S_{11}|^2)}{(1 - |\Gamma_1|^2)|1 - S_{22}\Gamma_r|^2} \tag{A6}$$

and

$$\eta_0 \equiv \frac{|S_{21}|^2}{1 - |S_{11}|^2}. \tag{A7}$$

For low-loss adapters both η and η_0 are close to 1, approaching 1 as the loss vanishes. Therefore, ζ must be close to 1, and it also must approach 1 as the loss vanishes. Furthermore, ζ is usually closer to 1 than η_0 because ζ describes the effects of reflections upon the adapter loss, and not primarily the loss itself. Equation (A7) shows that both reflective and dissipative adapter losses are contained in $|S_{21}|$ since the reflective loss, $1 - |S_{11}|^2$, must be divided out to get the dissipative efficiency η_0. These two types of losses are small in a good adapter. Hence, both $|S_{21}|$ and $|S_{11}|$ must be very accurately measured if (A7) is to be used to obtain η_0 by direct calculation. Connector imperfections can make such measurements difficult, but the SS technique circumvents these problems to a large extent because it measures efficiencies directly.

It is possible to rearrange ζ so that its reciprocal takes the form

$$\zeta^{-1}=1-\frac{2}{\left(1-|\Gamma_r|^2\right)}\operatorname{Re}\left[\Gamma_r S_{22}\overbrace{\left(1+\frac{S_{11}^* S_{21}^2/S_{22}}{1-|S_{11}|^2}\right)}^{0\text{ for lossless}}\right]$$
$$+\frac{2|\Gamma_r|^2|S_{21}|^2}{\left(1-|\Gamma_r|^2\right)\left(1-|S_{11}|^2\right)}\left[\underbrace{\frac{\left(1+|S_{22}|^2\right)\left(1-|S_{11}|^2\right)-|S_{21}|^4}{2|S_{21}|^2}}_{|S_{11}S_{22}|\text{ for lossless}}+|S_{11}S_{22}|\underbrace{\cos\theta}_{-1\text{ for lossless}}\right] \tag{A8}$$

where

$$\theta\equiv 2\phi_{21}-\phi_{11}-\phi_{22}. \tag{A9}$$

The quantities ϕ_{21}, ϕ_{11}, and ϕ_{22} are the phases of S_{21}, S_{11}, and S_{22} respectively.

The quantity in the overbrace of (A8) is small and approaches 0 as the adapter loss vanishes [6, p. 47]. The two quantities in the underbraces combine to give a value close to the quantity in the overbrace times $|S_{11}S_{22}|$. Consequently, the second term in (A8) is proportional to $|\Gamma_r S_{22}|$ times a small quantity, while the third term is proportional to $|\Gamma_r^2 S_{11}S_{22}|$ times approximately the same quantity. Therefore, the third term is much smaller than the second and can be discarded to obtain the following approximation:

$$\zeta\doteq 1+2\operatorname{Re}\left[\Gamma_r S_{22}\left(1+\frac{S_{11}^* S_{21}^2/S_{22}}{1-|S_{11}|^2}\right)\right]. \tag{A10}$$

Neither the phase of Γ_r nor the phase of the parenthetical expression in (A10) is known, so the sum of these phases can be any value from 0 to 2π. Therefore, ζ is uncertain by the second term of (A10) and leads to

$$\zeta=1\pm 2|\Gamma_r S_{22}|\left|1+\frac{S_{11}^* S_{21}^2/S_{22}}{1-|S_{11}|^2}\right|. \tag{A11}$$

The strict realizability conditions [6, pp. 46–47] for microwave networks and a considerable amount of manipulation lead to

$$|S_{22}|\left|1+\frac{S_{11}^* S_{21}^2/S_{22}}{1-|S_{11}|^2}\right|<(1-\eta_0)\left[|S_{22}|^2+(1-\eta_0')\right] \tag{A12}$$

where

$$\eta_0'\equiv\frac{|S_{21}|^2}{1-|S_{22}|^2} \tag{A13}$$

is the intrinsic efficiency of the adapter in its reverse direction. For a typical adapter $|S_{22}|^2$ is an order of magnitude less than $1-\eta_0'$. Furthermore, computer simulations show that the inequality in (A12) still holds in most cases if the first term on the right side is neglected. Therefore, dropping the $|S_{22}|^2$ compared to the $1-\eta_0'$ term, and setting $\eta_0'\doteq\eta_0$ yields

$$|S_{22}|\left|1+\frac{S_{11}^* S_{21}^2/S_{22}}{1-|S_{11}|^2}\right|<(1-\eta_0)^2. \tag{A14}$$

Finally, inserting (A14) into (A11) gives

$$\zeta=1\pm 2|\Gamma_r|(1-\eta_0)^2. \tag{A15}$$

Appendix II

The purpose of this appendix is to derive (A21) and (A24) and to show that $|A/B|$ is small.

Equation (A2) is a linear fractional transformation [9] of Γ_{ss} at reference plane 1 to Γ at reference plane 2 in Fig. 2. As such, it represents a circle in the complex or Argand plane, and can be expressed in the form

$$\Gamma=A+Be^{j\Psi} \tag{A16}$$

where [4]

$$A\equiv\frac{S_{22}+\sigma S_{11}^*|\Gamma_{ss}|^2}{1-|S_{11}\Gamma_{ss}|^2} \tag{A17}$$

and

$$B\equiv\frac{S_{21}^2|\Gamma_{ss}|}{1-|S_{11}\Gamma_{ss}|^2}. \tag{A18}$$

$|B|$ is the radius of the circle whose center is at A (Fig. 6). The phase angle Ψ is given by

$$\Psi\equiv\phi+2\arctan\left(\frac{|S_{11}\Gamma_{ss}|\sin(\phi+\phi_{11})}{1-|S_{11}\Gamma_{ss}|\cos(\phi+\phi_{11})}\right)$$
$$\doteq\phi+2|S_{11}\Gamma_{ss}|\sin(\phi+\phi_{11}) \tag{A19}$$

where ϕ is defined in (5). For a $|S_{11}|$ of 0.1 or less, Ψ and ϕ agree within 6° (arctan 0.1). (Although (A16) through (A19) are shown specifically for $|\Gamma_{ss}|$, they apply in general to any reflection coefficient at the input of the adapter.)

Equation (A18) can be combined with the definition (A7) to obtain

$$\eta_0=\frac{|B|}{|\Gamma_{ss}|}\left(\frac{1-|S_{11}\Gamma_{ss}|^2}{1-|S_{11}|^2}\right). \tag{A20}$$

The parenthetical factor in (A20) is close to 1 in most practical applications. For example, this factor is 1.0001 or 0.0004 dB for a $|\Gamma_{ss}|$ and an $|S_{11}|$ of 0.98 and 0.05 respectively. Therefore, setting

$$\eta_0\doteq\frac{|B|}{|\Gamma_{ss}|} \tag{A21}$$

leads to little error.

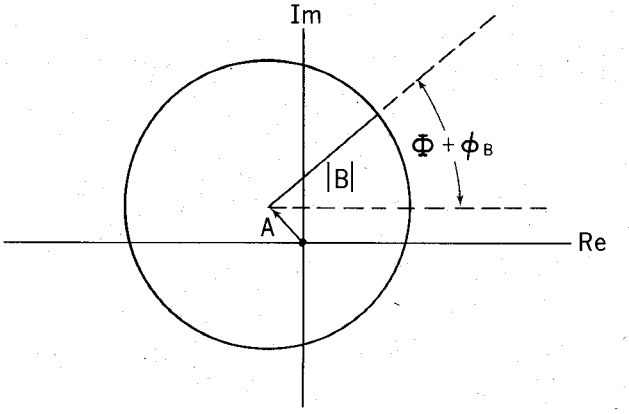

Fig. 6. An Argand diagram for A and B.

Taking the magnitude squared of (A16) leads to

$$|\Gamma|^2 = |A|^2 + |B|^2 + 2|AB|\cos(\Psi - \phi_A + \phi_B). \quad \text{(A22)}$$

The phase angle of Γ is given by

$$\phi_\Gamma = \arctan\left[\frac{|A|\sin\phi_A + |B|\sin(\Psi + \phi_B)}{|A|\cos\phi_A + |B|\cos(\Psi + \phi_B)}\right] \doteq \Psi + \phi_B \doteq \phi + \phi_B. \quad \text{(A23)}$$

The first approximation is good to 0.2 percent for a typical adapter. Combining (A22) and (A23) gives

$$|\Gamma|^2 = |A|^2 + |B|^2 + 2|AB|\cos(\phi_\Gamma - \phi_A). \quad \text{(A24)}$$

Note from (A19) and (A23) that ϕ_Γ and ϕ vary in the same manner.

The magnitude of A can be shown to be small by the following argument. From (A17) and (A3),

$$|A| = \frac{1-|S_{11}|^2}{1-|S_{11}\Gamma_{ss}|^2}\left|S_{22} + \frac{S_{21}^2 S_{11}^*}{1-|S_{11}|^2} - \frac{\sigma S_{11}^*(1-|\Gamma_{ss}^2|)}{1-|S_{11}|^2}\right| \doteq \left|S_{22} + \frac{S_{21}^2 S_{11}^*}{1-|S_{11}|^2} - S_{21}^2 S_{11}^*(1-|\Gamma_{ss}|^2)\right|. \quad \text{(A25)}$$

It follows from (A25) that

$$|A| < \left|S_{22} + \frac{S_{21}^2 S_{11}^*}{1-|S_{11}|^2}\right| + |S_{11}|(1-|\Gamma_{ss}|^2) \quad \text{(A26)}$$

where the $|S_{21}|^2$ factor in the last term of (A25) is close to 1 and therefore dropped. Finally, inserting (A14) into (A26) gives

$$|A| < (1-\eta_0)^2 + |S_{11}|(1-|\Gamma_{ss}|^2). \quad \text{(A27)}$$

Then, combining (A27) and (A21) leads to

$$\left|\frac{A}{B}\right| < \frac{(1-\eta_0)^2 + |S_{11}|(1-|\Gamma_{ss}|^2)}{\eta_0|\Gamma_{ss}|}. \quad \text{(A28)}$$

Measurements show that (A28) is a conservative estimate for the upper bound to the ratio $|A/B|$.

ACKNOWLEDGMENT

The authors wish to thank F. Clague for many valuable suggestions concerning the preparation of the manuscript.

REFERENCES

[1] R. W. Beatty, G. F. Engen, and W. J. Anson, "Measurement of reflections of waveguide joints and connectors using microwave reflectometer techniques," *IRE Trans. Instrum.*, vol. I-9, pp. 219–226, Sept. 1960.

[2] G. Almassy, "A first order correction to sliding short behavior with application to the problem of measuring small losses," *IEEE Trans. Instrum. Meas.*, vol. IM-20, pp. 162–169; Aug. 1970.

[3] G. F. Engen, "An extension to the sliding short method of conector and adapter evaluation," *J. Res. Nat. Bur. Stand.*, vol. 75C, pp. 177–183, Dec. 1971.

[4] G. F. Engen, "Calibration technique for automated network analyzers with application to adapter evaluation," *IEEE Trans. Microwave Theory Tech.*, vol. MTT-22, Dec. 1974.

[5] G. F. Engen, "An Introduction to the Description and Evaluation of Microwave Systems Using Terminal Invariant Parameters," Nat. Bur. Stands. Mono. 112, Oct. 1969.

[6] D. M. Kerns and R. W. Beatty, *Basic Theory of Waveguide Junctions and Introductory Microwave Circuit Analysis*. New York: Pergamon Press, 1967.

[7] *IEEE Standard Dictionary of Electrical and Electronic Terms*. New York: Wiley, 1972.

[8] G. F. Engen, "An improved circuit for implementing the six-port technique of microwave measurements," *IEEE Trans. Microwave Theory Tech.*, vol. MTT-25, Dec. 1977.

[9] R. V. Churchill, *Introduction to Complex Variables and Applications*. New York: McGraw-Hill, 1948.

William C. Daywitt was born in Denver, CO, on September 30, 1935. He received the B.S. degree in engineering physics in 1958 and the M.S. degree in applied mathematics in 1959, both from the University of Colorado, Boulder, where he completed most of the graduate work towards the Ph.D. degree in physics.

He joined the staff of the National Bureau of Standards (now NIST) in October 1959. He is currently with the Electromagnetic Fields Division, Center for Electronics and Electrical Engineering, in Boulder working in the area of microwave noise.

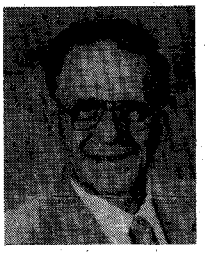

George Counas was born in July 1935. After serving in the U.S. Air Force, he joined the staff at the Boulder Laboratories of the National Bureau of Standards. Over the past 30 years he has worked in the Microwave Attenuation and Microwave Impedance Calibration Laboratories, the Remote Sensing Section, and the Microwave Noise Calibration Laboratory.